

Wave Transport in disordered waveguides: closed channel contributions and the coherent and diffuse fields

M. Yépez

Departamento de Física, Universidad Autónoma Metropolitana-Iztapalapa, Apartado Postal 55-534, 09340 México Distrito Federal, Mexico

Abstract. We study the wave transport through a disordered system inside a waveguide. The expectation value of the complex reflection and transmission coefficients (the coherent fields) as well as the transmittance and reflectance are obtained numerically. The numerical results show that the averages of the coherent fields are only relevant for direct processes, while the transmittance and reflectance are mainly dominated by the diffuse intensities, which come from the statistical fluctuations of the fields.

Keywords: Disordered waveguides; Quantum transport; Random processes

PACS: 72.80.Ng, 73.23.-b, 73.23.Ad, 42.25.Dd

INTRODUCTION

The wave transport through disordered systems has been of great interest in many fields of physics, where the wave interference phenomena plays a transcendental role [1–8]. The interference phenomena that occur when a wave propagates through a disordered medium containing a random distribution of scatterers is so complex that any change in the microscopic realization of the disorder modifies completely the interference pattern of a macroscopic observable [9]; therefore, only a statistical description makes sense. The complexity derives from the fluctuations in the refractive index as in disordered dielectric medium, the randomness of the scattering potentials, as in the case of disordered conductors with impurities or more in general, in disordered waveguides; the complexity not only derives from the randomness of the system, it is also consequence of the multiple scattering processes. In the present work we focus the study in the domain of disordered waveguides and in the quantum mechanics context (electron or scalar waves), nevertheless, the method could be applied to classical waves: electromagnetic or elastic waves.

Some previous studies in *quasi-one dimensional* (Q1D) disordered systems have found remarkable regularities for the statistical properties of wave transport in the sense that the statistic of macroscopic observables involves a rather small physical parameters, the *mean free paths* (MFPs). Those models are in good agreement with the scaling approaches [10–15], including the celebrated Dorokhov-Mello-Pereyra-Kumar (DMPK) [10, 16] and the non linear sigma-model [17–19] approaches.

Most of previous works were mainly focus on the study of the statistics of the transport coefficients, i.e., the transmittances, reflectances and the dimensionless conductance (transmission intensity), while the statistical properties of the complex coefficients or *coherent fields*, were not studied in detail; moreover, in those previous approaches, the closed channels or evanescent waves are not included in the description. For instance, the DMPK approach describes successfully the statistical properties of the conductance, where the only relevant physical parameter is the transport or elastic mean free path ℓ ; however, the DMPK model is not suitable to describe the statistics of the complex transmission and reflection coefficients. The models developed in Refs. [13, 14] give a more general description than the DMPK approach. In those models, the macroscopic statistics only depends on the channel-channel mean free paths ℓ_{aa_0} and the scattering mean free path ℓ_{a_0} : a and a_0 denote, respectively, the modes or channels of the incoming and outgoing waves. In principle, the approaches given Refs. [13, 14] are appropriate to describe the statistics of the coherent fields; however, those models do not consider the closed contributions, which, as it is demonstrated in Ref. [20], play a transcendental role in the statistical properties of the complex transmission and reflection coefficients.

In the present work we analyze numerically the influence of the closed channels in the macroscopic statistics of disordered waveguides. We present numerical results for the expectation values of the complex reflection and transmission coefficients, as well as of the corresponding intensities. In addition, we also present numerical simulations for coherent and diffuse intensities, which have not been studied in detail in previous theoretical and numerical studies. For that purpose we will use the *extended or generalized scattering matrix* (GSM) technique [8, 21–24].

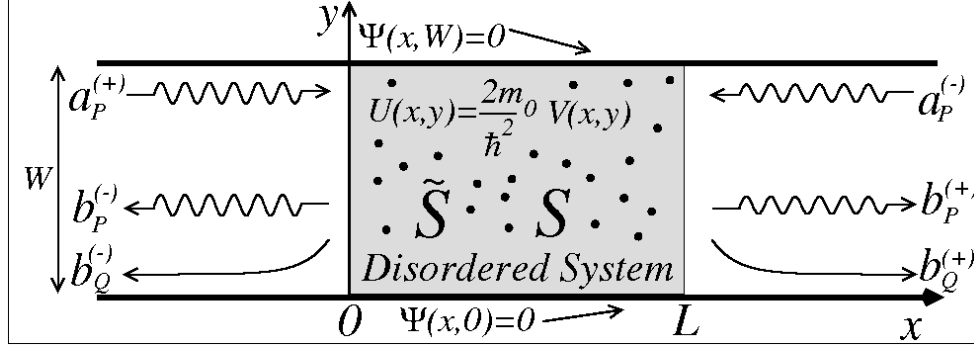


FIGURE 1. Scattering problem in a waveguide. $a_P^{(+)}$ and $a_P^{(-)}$ denote N dimensional vectors, being their elements all possible incoming open channel amplitudes. Analogously $b_P^{(-)}$ and $b_P^{(+)}$ are vectors with all possible outgoing open channel amplitudes and $b_Q^{(-)}$, $b_Q^{(+)}$, are the corresponding outgoing closed channel vectors, whose dimensionality N' is, in principle, infinite.

STATISTICAL SCATTERING PROPERTIES OF DISORDERED WAVEGUIDES

Generalized and reduced scattering matrices

Consider a two dimensional disordered system of uniform cross section and length L inside a waveguide with impenetrable walls, a constant width W , that is clean at both sides of the disordered region (see Fig. 1). The disordered system, which hereafter shall be called the *Building Block* (BB), is represented by a random potential U , whose microscopic model is introduced in the next section. Inside the waveguide, the solution of the wave equation $\nabla^2 \Psi + k^2 \Psi = U \Psi$ (k being the wavenumber in the clean region) is written as a series of traveling and evanescent waves, which are associated to *open and closed channels*, respectively. The waveguide supports precisely N open channels or traveling modes when $N < kW/\pi < N + 1$, while the number of closed channels or evanescent modes N' is, in principle, infinite.

In Fig. 1 it is shown the most general situation of the scattering problem, where incoming-waves of open channels $a_P^{(+)}$ and $a_P^{(-)}$ [incoming-waves in closed channels are not allowed, so $a_Q^{(+)} = a_Q^{(-)} = 0$], are scattered by the disordered system, giving rise to outgoing-waves, both in open channels (traveling modes) $b_P^{(+)}$, $b_P^{(-)}$ as in closed channels (evanescent modes) $b_Q^{(+)}$, $b_Q^{(-)}$; the symbols $+$ and $-$ denote, respectively, waves traveling to the right and to the left, while P and Q represent open and closed channel components, respectively. The scattering problem is formally described by GSM \tilde{S} [8], which relates open and closed channel outgoing-wave amplitudes to the open channels incoming-wave amplitudes, i.e.,

$$\begin{pmatrix} b_P^{(-)} \\ b_Q^{(-)} \\ b_P^{(+)} \\ b_Q^{(+)} \end{pmatrix} = \tilde{S} \begin{pmatrix} a_P^{(+)} \\ a_Q^{(+)} = 0 \\ a_P^{(-)} \\ a_Q^{(-)} = 0 \end{pmatrix}, \quad \text{with} \quad \tilde{S} = \begin{pmatrix} \tilde{r} & \tilde{t}' \\ \tilde{t} & \tilde{r}' \end{pmatrix}. \quad (1)$$

Even though the \tilde{S} matrix describes completely the scattering problem, it is important to notice that the closed channel amplitudes $b_Q^{(-)}$, $b_Q^{(+)}$ decrease exponentially as we move away from the disordered system, which is shown schematically in Fig. 1; moreover, those amplitudes do not contribute to the flux density current. For this reason, the scattering problem is usually described in terms of the well known *open channels* or *reduced scattering matrix* S , that relates open channel outgoing- and incoming-wave amplitudes in the asymptotic region, i.e.,

$$\begin{pmatrix} b_P^{(-)} \\ b_P^{(+)} \end{pmatrix} = S \begin{pmatrix} a_P^{(+)} \\ a_P^{(-)} \end{pmatrix}, \quad \text{with} \quad S = \begin{pmatrix} r & t' \\ t & r' \end{pmatrix}. \quad (2)$$

Generalized scattering matrix technique

In order to study the statistical scattering properties of the BB, we consider an initial condition in which an incoming-wave in the open channel a_0 travels from left to right, so that the outgoing-waves (backward and forward) are generated in any possible open channel $a = 1, \dots, N$: from now on a_0 and a will only denote, respectively, the incoming and outgoing open channels. Under this initial condition, we are interested in the statistics of observables related to the complex reflection r_{aa_0} ($\in r$) and transmission t_{aa_0} ($\in t$) coefficients as well as the corresponding reflectance $R_{aa_0} = |r_{aa_0}|^2$ and transmittance $T_{aa_0} = |t_{aa_0}|^2$, and the dimensionless conductance $g = \sum_{a,a_0}^N T_{aa_0}$, which has been widely studied.

The statistical scattering properties of the BB, are obtained numerically from an ensemble, where each member represents any possible microscopic realization of the disorder. For instance, the expectation values $\langle r_{aa_0} \rangle$, $\langle t_{aa_0} \rangle$, $\langle R_{aa_0} \rangle$ and $\langle T_{aa_0} \rangle$ are calculated as the average over the ensemble, where the *generalized scattering matrix technique* is used. To illustrate how this method is implemented, it is important to notice that each element of the reduced matrix S , Eq. (2), is extracted from the generalized matrix \tilde{S} , Eq. (1), which in turn is calculated by combining the generalized scattering matrices of the individual scatters of the system: see details of the combination law in Ref. [8]. The combination law captures any possible open or closed channel transition, which are result of the multiple scattering processes inside the disordered system. Once the reduced matrix S is known, the complex reflection r_{aa_0} and transmission t_{aa_0} coefficients, as well as the corresponding reflectance $R_{aa_0} = |r_{aa_0}|^2$ and transmittance $T_{aa_0} = |t_{aa_0}|^2$, are easily calculated. This procedure is repeated numerically for each microscopic realization of the ensemble, what allows us to generate an ensemble of matrices S and consequently to obtain, numerically, the ensemble averages $\langle r_{aa_0} \rangle$, $\langle t_{aa_0} \rangle$, $\langle R_{aa_0} \rangle$ and $\langle T_{aa_0} \rangle$.

The implementation of the GSM method mentioned above, exhibits that the closed channel or evanescent waves contribute implicitly to the S matrix given in Eq. (2). For this reason the S matrix of any realization of the microscopic disorder - and consequently the statistical properties associated to S - depend formally on the closed channels, which in general are neglected in the theoretical studies of quasi one dimensional (Q1D) disordered systems.

The GSM method also guaranties the flux conservation property $S^\dagger S = I$, which imposes the condition

$$T_{a_0} + R_{a_0} = 1, \quad (3)$$

being

$$T_{a_0} = \sum_{a=1}^N T_{aa_0}, \quad R_{a_0} = \sum_{a=1}^N R_{aa_0}, \quad (4)$$

the total transmittance T_{a_0} and reflectance R_{a_0} , respectively; the additions on a is over any possible outgoing open channel. Since any microscopic realization of the disorder satisfies the flux conservation property, Eq. (3), then the statistical properties will also be consistent with this general condition.

Coherent and diffuse fields

For a given realization of the microscopic disorder the complex coefficients of the transmitted and reflected waves can be written as the sum of the average $\langle t_{aa_0} \rangle$, $\langle r_{aa_0} \rangle$ (coherent) and residual Δt_{aa_0} , Δr_{aa_0} (diffuse) fields, i.e.,

$$t_{aa_0} = \langle t_{aa_0} \rangle + \Delta t_{aa_0}, \quad \langle \Delta t_{aa_0} \rangle \equiv 0, \quad (5)$$

$$r_{aa_0} = \langle r_{aa_0} \rangle + \Delta r_{aa_0}, \quad \langle \Delta r_{aa_0} \rangle \equiv 0. \quad (6)$$

Δt_{aa_0} , Δr_{aa_0} give the statistical fluctuations around the corresponding coherent fields $\langle t_{aa_0} \rangle$, $\langle r_{aa_0} \rangle$. In a similar way, the transmittance and reflectance of a given realization are written in the following way:

$$T_{aa_0} = |t_{aa_0}|^2 = \langle T_{aa_0} \rangle + \Delta T_{aa_0}, \quad \langle \Delta T_{aa_0} \rangle \equiv 0, \quad (7)$$

$$R_{aa_0} = |r_{aa_0}|^2 = \langle R_{aa_0} \rangle + \Delta R_{aa_0}, \quad \langle \Delta R_{aa_0} \rangle \equiv 0, \quad (8)$$

where

$$\langle T_{aa_0} \rangle = \langle |t_{aa_0}|^2 \rangle + \langle |\Delta t_{aa_0}|^2 \rangle, \quad (9)$$

$$\langle R_{aa_0} \rangle = \langle |r_{aa_0}|^2 \rangle + \langle |\Delta r_{aa_0}|^2 \rangle, \quad (10)$$

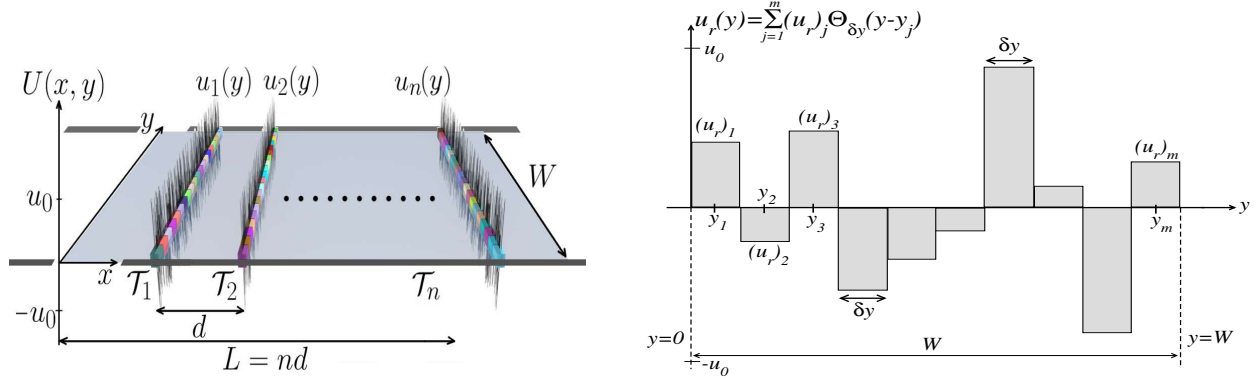


FIGURE 2. Left: Schematic representation of the building block as sequence of “thin” δ -potential slices. Right: Profile of the transverse dependence $u_r(y)$, Eq. (15), of the r th scattering unit. The random values $(u_r)_j$ were generated by using the uniform distribution of Eq. (14).

denote, respectively, the expectation values of the transmittance and reflectance coefficients, while

$$\Delta T_{aa_0} = |\Delta t_{aa_0}|^2 - \langle |\Delta t_{aa_0}|^2 \rangle + 2\text{Re}(\langle t_{aa_0} \rangle \Delta t_{aa_0}^*), \quad (11)$$

$$\Delta R_{aa_0} = |\Delta r_{aa_0}|^2 - \langle |\Delta r_{aa_0}|^2 \rangle + 2\text{Re}(\langle r_{aa_0} \rangle \Delta r_{aa_0}^*), \quad (12)$$

give the corresponding statistical fluctuations. Equations (9) and (10) show that the ensemble average of the transmittance $\langle T_{aa_0} \rangle$ and reflectance $\langle R_{aa_0} \rangle$ are constituted of two different contributions: the coherent intensities $|\langle t_{aa_0} \rangle|^2$, $|\langle r_{aa_0} \rangle|^2$ and the diffuse intensities $\langle |\Delta t_{aa_0}|^2 \rangle$, $\langle |\Delta r_{aa_0}|^2 \rangle$.

POTENTIAL MODEL FOR THE BUILDING BLOCK

The Building Block is represented by a random potential $U(x, y)$ (in units of k^2), that is constructed as a sequence of n ($\gg 1$) statistically independent and identically distributed scattering units, which are separated from each other by a fixed distance d in the wave propagation direction x [see Fig. 2 (left)]. The scattering properties of a scattering unit, are described by means of its extended scattering matrix \tilde{s}_r , which is proportional to the so called *transition matrix* \mathcal{T}_r , that captures any possible channel-channel transition [25–27]. The thickness of each scattering unit is much smaller than the distance d , which in turn is much smaller than the wavelength λ . The r th scattering unit ($r = 1, 2, \dots, n$) centered at $x_r = rd$, is specified by its potential $U_r(x, y)$ (in units of k^2), that is approximated as a delta potential slice in the longitudinal direction x , with random strength $u_r(y)$ (in units of k) in the transverse direction y ; therefore, the BB is a system of length $L = nd$ given by the following potential model:

$$U(x, y) = \sum_{r=1}^n U_r(x, y) = \sum_{r=1}^n u_r(y) \delta(x - x_r). \quad (13)$$

The microscopic model of a delta slice that is used in the present work is shown in Fig. 2 (right), where the transverse dependence of the r th slice $u_r(y)$, Eq. (13), is generated in the following way: i) The width of the waveguide W is divided into $m \gg 1$ segments all of them with the same length $\delta y = W/m \ll \lambda$ (being λ the wavelength). ii) The j th ($j = 1, 2, \dots, m$) segment is centered at $y_j = (j - 1/2)\delta y$ and is defined by the interval $y \in [(j - 1)\delta y, j\delta y]$. iii) Inside each interval the function $u_r(y)$ takes a constant potential value $(u_r)_j$, which is sampled from the uniform distribution

$$P(u_r) = \frac{1}{2u_0}, \quad (u_r)_j \in [-u_0, u_0]. \quad (14)$$

The procedure explained above generates the random profile for the r th scattering unit, which is mathematically represented by the expression

$$u_r(y) = \sum_{j=1}^m (u_r)_j \Theta_{\delta y}(y - y_j), \quad (15)$$

where the $\Theta_{\delta y}(y - y_j)$ is the finite step function that takes the value 1 if $y \in [y_j - \delta y/2, y_j + \delta y/2]$ and zero if otherwise.

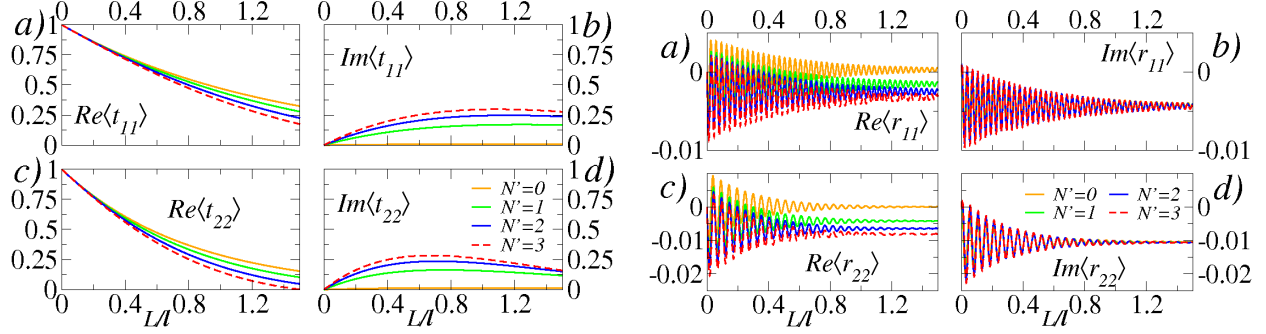


FIGURE 3. Numerical results for $\langle t_{aa_0} \rangle$ (left) and $\langle r_{aa_0} \rangle$ (right) vs L/ℓ . Each simulation considers $N = 2$ propagating modes and several evanescent modes ($N' = 0, 1, 2, 3$).

NUMERICAL RESULTS

In this section we present numerical results for the expectation values $\langle t_{aa_0} \rangle$, $\langle r_{aa_0} \rangle$, $\langle T_{aa_0} \rangle$ and $\langle R_{aa_0} \rangle$ of the BB. The aim is to study their evolution with L and the role of the closed channels in the statistical scattering properties of the Building Block. The influence of the closed channels is analyzed numerically by considering four numerical simulations for the expectation values of interest. These simulations are performed for a waveguide that supports $N = 2$ open channels (with $kW/\pi = 2.5$), but each simulation takes into account $N' = 0, 1, 2, 3$ closed channels in the calculations, respectively. The numerical expectation values $\langle t_{aa_0} \rangle$, $\langle r_{aa_0} \rangle$, $\langle T_{aa_0} \rangle$, and $\langle R_{aa_0} \rangle$, are obtained as the average over an ensemble of 10^6 realizations of the microscopic disorder, where the scattering matrix of each realization is generated by using the potential model of the previous section and the GSM method introduced in the second section. As in previous works, the numerical expectation values will be plotted as function of the dimensionless length L/ℓ , ℓ being the transport mean free path.

The numerical results of Fig. 3 (left) show that $\text{Re}\langle t_{aa_0} \rangle$ decreases as L/ℓ increases; this behavior becomes more notorious as the number of closed channels ($N' = 0, 1, 2, 3$) considered in the calculations is increased. This figure also shows that the influence of the closed channels in $\text{Im}\langle t_{aa_0} \rangle$ is even more dramatic: if closed channels are not included in the numerical simulations ($N' = 0$), $\text{Im}\langle t_{aa_0} \rangle$ is small ($\sim 10^{-2}$), but not strictly zero; however, when the closed channels are considered ($N' = 1, 2, 3$), $\text{Im}\langle t_{aa_0} \rangle$ increases one order of magnitude.

In the right panel of Fig. 3 we can appreciate a remarkable oscillatory behavior for $\langle r_{aa_0} \rangle$, which is rapidly attenuated as L/ℓ increases, regardless the number of closed channels that are considered in the calculation. The phase and amplitude of $\langle r_{aa_0} \rangle$ depend little on the closed channels contributions. However, the most notorious dependence on the closed channel contributions is exhibited by $\text{Re}\langle r_{aa_0} \rangle$, whose oscillations are given around a “background” that depends on the number of closed channels considered in the calculations; in contrast, the four simulations of $\text{Im}\langle r_{aa_0} \rangle$ seem to oscillates around the same “background,” no matter how many closed channels were used in the calculations.

Most of previous theoretical models cannot describe the numerical evidence shown in Fig. 3 for $\langle t_{aa_0} \rangle$ and $\langle r_{aa_0} \rangle$, due to the absence of closed channels. As an example, we consider Mello-Tomsovic (MT) prediction [13] for the expectation values of the coherent fields

$$\langle t_{aa_0} \rangle^{(\text{MT})} = \delta_{aa_0} e^{-L/\ell_{a_0}}, \quad (16)$$

$$\langle r_{aa_0} \rangle_L^{(\text{MT})} = 0, \quad (17)$$

where ℓ_{a_0} is the scattering mean free path of the incoming open channel a_0 . We have verified that the MT prediction $\langle t_{aa_0} \rangle^{(\text{MT})} = e^{-L/\ell_{a_0}}$ is indistinguishable from the numerical result of $\text{Re}\langle t_{aa_0} \rangle$ when the closed channels are not considered in the calculation. However, once the closed channels are included ($N' = 1, 2, 3$), $\text{Re}\langle t_{aa_0} \rangle$ decreases faster than MT predicts, Eq. (16). In addition, the behavior $\text{Im}\langle t_{aa_0} \rangle \neq 0$ is not predicted by MT result. On the other hand, although the numerical results of Fig. 3 (right) show that the amplitude of the oscillation of $\langle r_{aa_0} \rangle$ is small ($\sim 10^{-2}$), this expectation value is not zero, even when the closed channels are not included; therefore, the MT prediction $\langle r_{aa_0} \rangle^{(\text{MT})} = 0$ is not able to describe the numerical results shown in right panel of Fig. 3.

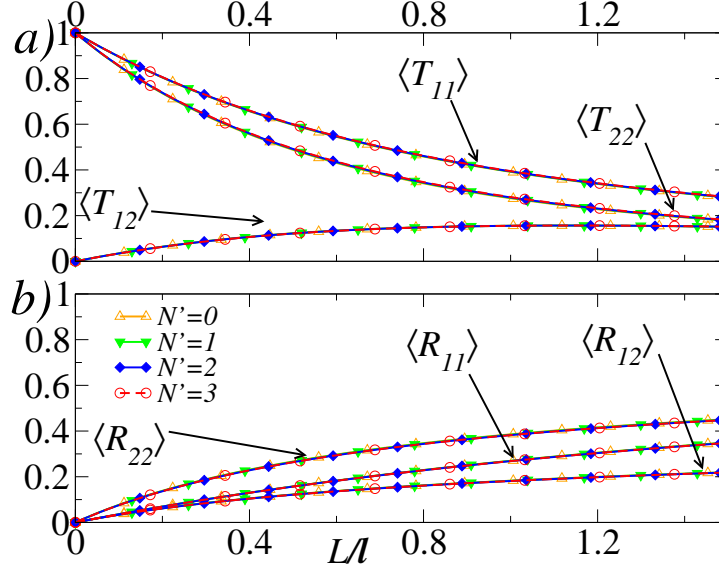


FIGURE 4. Numerical results for $\langle T_{aa_0} \rangle$ and $\langle R_{aa_0} \rangle$ vs L/ℓ . Each simulation considers $N = 2$ propagating modes and different evanescent modes ($N' = 0, 1, 2, 3$).

In previous studies [28, 29], it has been shown that the coherent wave fields are characterized by an effective wave number k_{eff} , whose real part determines the phase of the coherent field, while its imaginary part represents the losses due to scattering (often known as waveguide extrinsic losses). As the wave propagates, the amplitude of the coherent part decays exponentially with the length L of the system. However, in a recent study [20] it has been theoretically demonstrated that the exponential decay of the coherent fields $\langle t_{aa_0} \rangle$ and $\langle r_{aa_0} \rangle$ is strongly modified when the closed channels are correctly taken into account: changes in the phase of the coherent field (i.e. in the real part of the effective wave number) are solely related to evanescent modes, while the scattering mean free path ℓ_{a_0} is insensitive to the closed channel inclusion. This prediction given in Ref. [20] allows us to understand the intriguing numerical results shown in Fig. 3.

In Fig. 4, we present the complete set of numerical expectation values of the transmittance $\langle T_{aa_0} \rangle$ and reflectance $\langle R_{aa_0} \rangle$. From this figure, we can appreciate that the closed channels do not have any effect in the expectation values $\langle T_{aa_0} \rangle$ and $\langle R_{aa_0} \rangle$. In a similar way, Fig. 5 shows that the expectation values of the total transmittance $\langle T_{a_0} \rangle = \sum_{a=1}^N \langle T_{aa_0} \rangle$ and reflectance $\langle R_{a_0} \rangle = \sum_{a=1}^N \langle R_{aa_0} \rangle$, as well as the dimensionless conductance $\langle g \rangle = \sum_{a,a_0=1}^N \langle T_{aa_0} \rangle = \sum_{a_0=1}^N \langle T_{a_0} \rangle$, are also insensitive to the closed channel contributions. In Fig. 5, we can also appreciate that the numerical expectation values $\langle T_{a_0} \rangle$ and $\langle R_{a_0} \rangle$ satisfy the flux conservation property, Eq. (3), i.e., $\langle T_{a_0} \rangle + \langle R_{a_0} \rangle = 1$; therefore, the numerical results are consistent with the flux conservation property.

The numerical evidence shown in Figs. 4 and 5, confirms previous numerical results, where the closed channels do not contribute in the statistics of transport coefficients [14]. This evidence justifies the omission of the closed channels in the description of the statistical properties of the transport coefficients T_{aa_0} and R_{aa_0} , which is a common approximation in the theoretical study of wave transport through disordered systems. The no role of the closed channels in the statistics of the transport coefficients T_{aa_0} , R_{aa_0} and g , is theoretically explain in Ref. [20], where it is demonstrated that the statistical properties of the transmittance and the reflectance only depends on the scattering mean free path ℓ_{a_0} , in which the closed channels play no role.

In contrast with the numerical results shown in Fig. 3 for the coherent fields $\langle t_{aa_0} \rangle$ and $\langle r_{aa_0} \rangle$, the expectation values of the transmittance $\langle T_{aa_0} \rangle$ and reflectance $\langle R_{aa_0} \rangle$ are insensitive to the closed channel influence, which means that both, coherent $|\langle t_{aa_0} \rangle|^2$, $|\langle r_{aa_0} \rangle|^2$ and diffuse $|\langle \Delta t_{aa_0} \rangle|^2$, $|\langle \Delta r_{aa_0} \rangle|^2$ intensities, Eqs. (9)-(10), are insensitive to the closed channel contributions. In order to analyze the closed channel influence in both kinds of intensities, in Fig. 6 we plotted the ensemble average of the transport coefficients $\langle T_{22} \rangle$, $\langle R_{22} \rangle$ and the corresponding coherent intensities $|\langle t_{22} \rangle|^2$, $|\langle r_{22} \rangle|^2$. Fig. 6(a) shows that the coherent field intensity $|\langle t_{22} \rangle|^2$ becomes less important for large values of L/ℓ , where the diffuse field governs the behavior of $\langle T_{22} \rangle$. In contrast, Fig. 6(b) shows that the diffuse field $|\langle \Delta r_{22} \rangle|^2$ dominates the behavior of $\langle R_{22} \rangle$ for all L/ℓ .

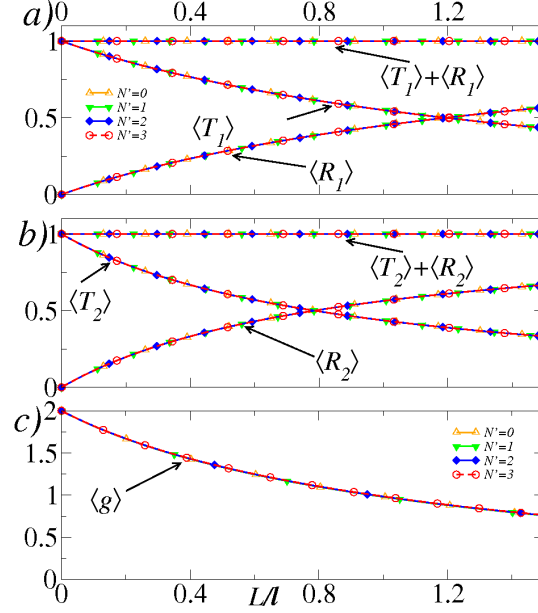


FIGURE 5. Panels (a) and (b) shows the numerical expectation values of the total transmittance $\langle T_{a_0} \rangle$ and reflectance $\langle R_{a_0} \rangle$; the flux conservation property $\langle T_{a_0} \rangle + \langle R_{a_0} \rangle = 1$ is also shown. In (c) it is shown the numerical expectation value of the dimensionless conductance $\langle g \rangle$. Each simulation considers $N = 2$ propagating modes and different evanescent modes ($N' = 0, 1, 2, 3$).

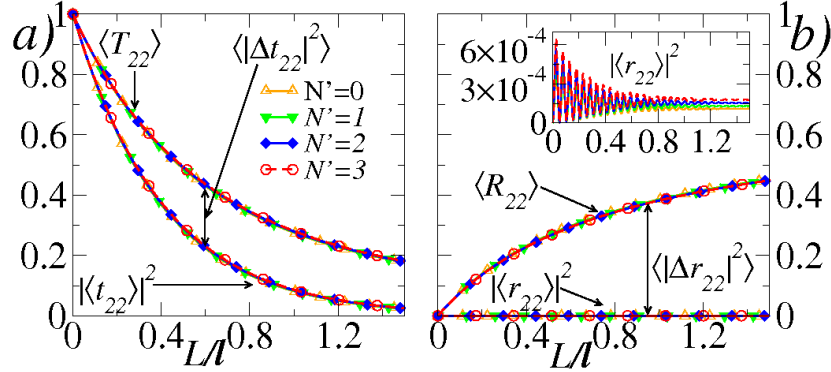


FIGURE 6. Numerical results for (a) the transmittance $\langle T_{22} \rangle$ and (b) the reflectance $\langle R_{22} \rangle$, and their coherent intensities $|\langle t_{22} \rangle|^2$, $|\langle r_{22} \rangle|^2$. Each simulation considers $N = 2$ propagating modes and different evanescent modes ($N' = 0, 1, 2, 3$).

CONCLUSIONS

We analyzed numerically the influence of the closed channels in the statistical scattering properties of disordered waveguides. Our numerical results show that the statistical average of the transmittance $\langle T_{aa_0} \rangle$, the reflectance $\langle R_{aa_0} \rangle$, and the dimensionless conductance $\langle g \rangle$ are insensitive to the closed channels inclusion, which is in good agreement with previous numerical simulations. In contrast, the expectation values of complex transmission and reflection coefficients, i.e., the coherent fields $\langle t_{aa_0} \rangle$, $\langle r_{aa_0} \rangle$ depend drastically on the closed channel contributions. Since the numerical results show that the coherent intensities $|\langle t_{aa_0} \rangle|^2$, $|\langle r_{aa_0} \rangle|^2$ do not depend strongly on the closed channels inclusion, then closed channels modify mainly the phases of the coherent fields $\langle t_{aa_0} \rangle$, $\langle r_{aa_0} \rangle$.

The numerical results also exhibit that the transmittance $\langle T_{aa_0} \rangle$ and the reflectance $\langle R_{aa_0} \rangle$ are mainly dominated by their corresponding diffuse $\langle |\Delta t_{aa_0}|^2 \rangle$, $\langle |\Delta r_{aa_0}|^2 \rangle$ intensities: the coherent intensity of the transmittance $|\langle t_{aa_0} \rangle|^2$, decreases rapidly as the length L of the disordered region increases, while the coherent intensity of the reflectance $|\langle r_{aa_0} \rangle|^2$ is negligible for any value of L .

ACKNOWLEDGMENTS

The author thanks J. Feilhauer, L. Froufe-Pérez, J. J. Sáenz and P. A. Mello for important discussions, and C. Lopez Nataren for technical support in the numerical simulations. This work has been supported by postdoctoral grants (No. 162768 and 187138) of the Mexican Consejo Nacional de Ciencia y Tecnología.

REFERENCES

1. R. Landauer, *Philosophical Magazine* **21**, 863–867 (1970).
2. A. Ishimaru, *Waves Propagation and Scattering in Random Media*, Academic Press, New York, 1978.
3. B. L. Al'tshuler, P. A. Lee, and R. A. Webb, editors, *Progress on Electron Properties of Metals*, North-Holland, 1991.
4. P. Sheng, *Introduction to Wave Scattering, Localization and Mesoscopic Phenomena*, Academic Press, New York, 1995.
5. Y. Imry, *Introduction to Mesoscopic Physics*, Oxford University Press, Oxford, 1997.
6. S. Datta, *Electronic Transport in Mesoscopic Systems*, Cambridge University Press, Cambridge, 1997.
7. C. W. J. Beenakker, *Rev. Mod. Phys.* **69**, 731–808 (1997).
8. P. A. Mello, and N. Kumar, *Quantum Transport in Mesoscopic Systems. Complexity and Statistical Fluctuations*, Oxford University Press, Oxford, 2010.
9. A. D. Stone, *Physics and Technology of Submicron Structures*, Springer-Verlag, Berlin, Heidelberg, 1988.
10. P. A. Mello, P. Pereyra, and N. Kumar, *Ann. Phys. (N.Y.)* **181**, 290 (1988).
11. P. A. Mello, and B. Shapiro, *Phys. Rev. B* **37**, 5860–5863 (1988).
12. L. S. Froufe-Pérez, P. García-Mochales, P. A. Serena, P. A. Mello, and J. J. Sáenz, *Phys. Rev. Lett.* **89**, 246403 (2002).
13. P. A. Mello, and S. Tomsovic, *Phys. Rev. B* **46**, 15963–15981 (1992).
14. L. S. Froufe-Pérez, M. Yépez, P. A. Mello, and J. J. Sáenz, *Phys. Rev. E* **75**, 031113 (2007).
15. J. Feilhauer, and M. Moško, *Phys. Rev. B* **83**, 245328 (2011).
16. O. N. Dorokhov, *JETP Lett.* **36**, 318 (1982).
17. K. B. Efetov, and A. I. Larkin, *JETP Lett.* **58**, 444 (1983).
18. Y. V. Fyodorov, and A. D. Mirlin, *Int. J. Mod. Phys. B* **8**, 3795 (1994).
19. P. W. Brouwer, and K. Frahm, *Phys. Rev. B* **53**, 1490 (1996).
20. M. Yépez, and J. J. Sáenz (2014), to be published.
21. J. A. Torres, and J. J. Sáenz, *Journal of the Physical Society of Japan* **73**, 2182–2193 (2004).
22. R. Mittra, and S. W. Lee, *Analytical Techniques in the Theory of Guided Waves*, MacMillan, New York, 1971.
23. R. Mittra, C. H. Chan, and T. Cwik, *Proceedings of the IEEE* **76**, 1593–1615 (1988).
24. A. Weisshaar, J. Lary, S. M. Goodnick, and V. K. Tripathi, *Journal of Applied Physics* **70**, 355–366 (1991).
25. A. Messiah, *Quantum Mechanics*, Dover, New York, 1999.
26. R. G. Newton, *Scattering Theory of Waves and Particles*, Springer-Verlag, New York, Heidelberg, Berlin, 1982.
27. P. Roman, *Advanced Quantum Theory*, Addison-Wesley, Massachusetts, 1965.
28. M. Lax, *Phys. Rev.* **85**, 621–629 (1952).
29. L. L. Foldy, *Phys. Rev.* **67**, 107–119 (1945).